Original Article

Author for correspondence:
Aysun Inal, Antalya Training and Research Hospital, Radiation Oncology Department, Antalya, Turkey. E-mail: aysuntoy@yahoo.com

CAMBRIDGE UNIVERSITY PRESS

Dosimetric evaluation of two phases of respiratory movement using a lung equivalent material for radiotherapy treatment planning

Aysun Inal [ORCID]

Antalya Training and Research Hospital, Radiation Oncology Department, Antalya, Turkey

Abstract

Background/aim: Radiation dosimetry requires special phantoms which are comparable with organs and tissues of a human body. The lung is one of the organs with a low density. Therefore, it is important to create and use lung equivalent phantoms in dosimetric controls. The aim of this study was to investigate the importance of using lung equivalent phantoms for different respiratory phases during measurements with both computed tomography (CT) and linear accelerator.

Materials and methods: The maximum lung inhalation phantom (LIP) and lung exhalation phantom (LEP) were created for two respiratory phases. The Hounsfield Unit (HU) values based on the selected slice thickness and CT tube voltages were investigated, as well as the difference between energy and algorithms used in the treatment planning system.

Results: It was found that the change in HU values according to slice thickness were more significant in measurements for respiratory phases. The dose difference between LEP and LIP at a point which is located 1 cm below the surface of the phantoms was found as 1·0% for 6 megavolt (MV) and 2·8% for 18 MV. The highest difference between the two algorithms was found to be 7·22% for 6 MV and 10·93% for 18 MV for LIP phantom.

Conclusion: It can be said that the LIP and LEP phantoms prepared in accordance with respiratory phases can be a simple and inexpensive method to investigate any difference in dosimetry during respiratory phases. Also, measured and calculated dose values are in good agreement when thinner slice thickness was chosen.

Introduction

The human body has a complex anatomy with regions of different density such as soft tissue, lungs, bones and organs containing air. Computed Tomography (CT) scans are used to determine the clinical and physical data of these organs before radiotherapy treatment planning for cancer patients. CT images contain the basic physical information such as size, shape and location of inhomogeneous structures, as well as electron densities (EDs) determined by Hounsfield Units (HUs) which are defined individually for each tissue.[1]

In radiation therapy, specific phantoms are required to simulate the organs and tissues of the human body. These phantoms enable the verification of congruity between the treatment planning systems (TPS) and dose distribution in the patient's body.[2–4] Lung is one of the most important low-density organs in the human body. Some commercial lung phantoms contain about 60% carbon, 10% hydrogen and 20% oxygen,[5] whereas healthy adult lung tissue contains approximately 10% carbon, 10% hydrogen and 75% oxygen.[6] This dissimilarity between the physical properties of commercial lung phantoms and human lung tissue is a proverbial issue. Some researchers have used corks of 0·2–0·4 g/cm^3 density with an expectation of representing normal lung tissue more accurately.[7] Chang et al.[5] report that the dosimetric properties of corks are very similar to lung tissue due to their physical properties and elemental composition. The natural movement of the lung occurs during inhalation and exhalation phases. The HU values are −814 and −735 in the upper part of the lung, and −819 and −720 in the lower part of the lung during inhalation and exhalation, respectively. Aarup et al.[8] have observed lung densities ranging from 0·1 to 0·4 g/cm^3 for deep inspiration breath-hold and end-expiration, respectively.

In radiotherapy treatment planning, optimisation is based on the requirement of the maximum dose to the target volume while minimising the dose to the surrounding normal tissue. Accurate determination of the dose distribution in the lung requires advanced dose calculation algorithms. The dose calculation by TPS frequently uses the convolution and superposition algorithms. The dosimetric predictors of radiation-induced lung complications are related to the dose distributions created by these algorithms.

Without any tissue-density correction, the actual dose in the tumour and normal tissue cannot be estimated accurately. In addition, the calculated dose depends on several different parameters such as energy, field size and the number of fields. In radiotherapy, treatment plans are
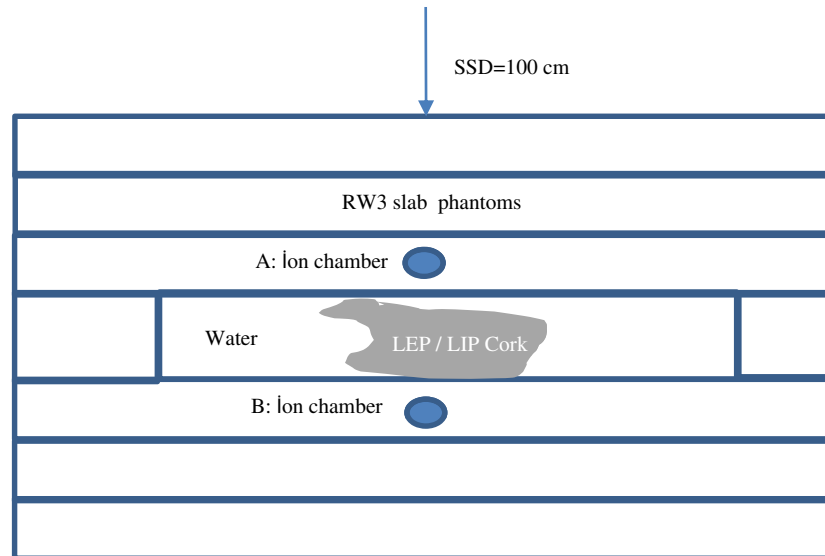
Figure 1. The set-up schema of LEP and LIP.

performed and evaluated on axial slices which were obtained in a static period. However, a normal human lung inhales 12 times per minute.

In this study, phantoms that are suitable for simulating maximum inhalation and exhalation phases were created. In these phases, HU values obtained based on the selected slice thickness and CT tube voltages, and also the difference between energy and used algorithms in treatment planning, were investigated. In addition, to investigate the effects of the patient's respiratory movement on absorbed dose, the calculations performed by TPS were confirmed via measurements from a linear accelerator (LinAc). For this purpose, a lung inhalation phantom (LIP) was prepared by increasing the amount of air in the lung and a lung exhalation phantom (LEP) was constructed by replacing the air volume with cork layers, as home-made phantoms. The usability of these phantoms to represent inhomogeneous structures employing different calculation parameters were investigated.

Materials and Method

In this study, axial slices of water and two lung equivalent phantoms were scanned by a CT device (GE-Light Speed 64, GE, United States) and the images were sent to the TPS (CMS Co., Ltd, St Louis, MO, United States) to obtain a treatment plan and the corresponding doses. The calculated doses were then compared with the measurements taken by Elekta Synergy Platform (Elekta, Crawley, UK) LinAc.

Ethical considerations

This study was approved by the Institutional Scientific Research Ethics Committee. All procedures were performed in accordance with the ethical standards of the institutional research committee and with the 1964 Helsinki Declaration and its later amendments or comparable ethical standards. Informed consent was waived owing to the retrospective chart review nature of the study.

Phantoms

For the LEP phantom, 15 cork pieces, each 2 mm thick, were placed in an oval cup of $8 \times 17 \times 5 \cdot 5$ cm^3 dimensions in such a way that there was no gap among the pieces. For the LIP phantom,

one-third of cork pieces were replaced by air. Both phantoms were fixed in a $30 \times 20 \times 3$ cm^3 container filled with water. The measurement set-up of the phantoms is shown in Figure 1. The third phantom with the same geometry was formed to contain only water having homogeneous structure, which was used as a control phantom. All three phantoms created in the clinic were home-made phantoms.

CT scan processes

Four different axial CT scan procedures were performed for the phantoms, each being performed at the same constant current of 130 mA but with different slice thicknesses and tube voltages as follows: slice thickness 0·625 mm and 80 kV tube voltage (0·625/80), 0·625 mm and 140 kV (0·625/140), 3·75 mm and 80 kV (3·75/80), and 3·75 mm and 140 kV (3·75/140). In the CT images, HU values were read at four different points selected along the centre axis (called as HU$_{mean}$) which were then sent to TPS for planning.

TPS processes

The outer frame of each image was first contoured in the TPS. Then, for each energy, the EDs corresponding to the HU values were plotted against the CT number (CT–ED) for 80 and 140 kV. The calculations were performed by using 6 and 18 megavolt (MV), for multiple fields (3×3, 4×4, 5×5, 10×10 and 20×20 cm^2) by convolution and superposition algorithms for three different phantoms. In calculations, the source–surface distance (SSD) was set to 100 cm. The doses corresponding to 100 Monitor Units (MU) were calculated for each field size.

LinAc processes

Before the measurements in LinAc, each energy was calibrated to have 1 cGy to be equal to 1 MU at the maximum dose point. Each of the three phantoms were placed between points A (1 cm over the phantom) and B (1 cm under the phantom), which have 0·6 cc cylindrical ion chamber (IBA, FC65-P cylindrical ion chamber), as shown in Figure 1 for scanning in CT. These points were chosen so as to find the effects of the respiratory phases on the central axis of the beam and close to the home-made phantoms. The measured

Table 1. The calculated absorbed doses (cGy) and percent differences in two algorithms and slice thicknesses/tube voltages for water

	Calculated absorbed dose for water (cGy)				
			Algorithm		
Energy	Slice thickness (mm)/ tube voltage (kV)	CP	Convolution	Superposition	Difference (%)
6 MV	0·625/80	A	461·3	460·1	0·26
		B	306·9	304·8	0·68
	0·625/140	A	462·5	460·7	0·39
		B	309·7	307·7	0·65
	3·75/80	A	463·7	462·3	0·30
		B	311·4	309	0·77
	3·75/140	A	462·8	462	0·17
		B	309·1	306·3	0·91
18 MV	0·625/80	A	475·9	471·3	0·97
		B	356·6	355·9	0·20
	0·625/140	A	475·1	471·7	0·72
		B	358·7	356·8	0·53
	3·75/80	A	476·7	473·4	0·69
		B	360·3	357	0·92
	3·75/140	A	475·6	471·7	0·82
		B	358·4	355·7	0·75

CP, calculated point; Difference %, the percent difference between two algorithms; cGy, centigray; MV, megavolt.

Table 2. The calculated absorbed doses (cGy) and percent differences in two algorithms and slice thicknesses/tube voltages for LEP

	Calculated absorbed dose for LEP (cGy)				
			Algorithm		
Energy	Slice thickness (mm)/ tube voltage (kV)	CP	Convolution	Superposition	Difference (%)
6 MV	0·625/80	A	462·4	465·6	0·69
		B	369·4	348·5	5·66
	0·625/140	A	465·1	466·5	0·30
		B	368	347·1	5·68
	3·75/80	A	464·4	465·9	0·32
		B	369	349·3	5·34
	3·75/140	A	465·2	465·9	0·15
		B	366·1	349	4·67
18 MV	0·625/80	A	476·6	461·5	3·17
		B	402·8	368·2	8·59
	0·625/140	A	476	459·3	3·51
		B	401·8	370	7·91
	3·75/80	A	478·2	459·9	3·83
		B	402·6	370·3	8·02
	3·75/140	A	478·3	458·9	4·06
		B	400·3	370·9	7·34

CP, calculated point; Difference %, the percent difference between two algorithms; cGy, centigray; MV, megavolt.

Table 3. The calculated absorbed doses (cGy) and percent differences in two algorithms and slice thicknesses/tube voltages for LIP

	Calculated absorbed dose for LIP (cGy)				
			Algorithm		
Energy	Slice thickness (mm)/ tube voltage (kV)	CP	Convolution	Superposition	Difference (%)
6 MV	0·625/80	A	460·2	462·1	0·41
		B	371·7	345·3	7·10
	0·625/140	A	460	461·7	0·37
		B	373·1	346·6	7·10
	3·75/80	A	463·5	464·2	0·15
		B	371·3	348·6	6·11
	3·75/140	A	462	461·2	0·17
		B	372·4	345·5	7·22
18 MV	0·625/80	A	473·6	465·2	1·77
		B	404·6	362·1	10·50
	0·625/140	A	473·7	467·1	1·39
		B	403·6	359·5	10·93
	3·75/80	A	476·5	464·3	2·56
		B	404·5	366·6	9·37
	3·75/140	A	453·5	464	2·32
		B	383·5	362·8	5·40

CP, calculated point; Difference %, the percent difference between two algorithms; cGy, centigray; MV, megavolt.

values obtained with electrometer (Dose1, IBA) were then converted to absorbed dose by using calibration factors and temperature–pressure corrections.

Results

The HU_{mean} values in the axial slices of the water-phantom were similar according to the applied tube voltage (kV) and slice thickness (HU_{mean} ± std.deviation=1·00 ± 10 for both kV and slice thickness). For the LIP, the HU_{mean} value increased (−848·50 ± 47 and −841·78 ± 61 for 80 and 140 kV, respectively) with increasing kV. Also, by increasing the slice thickness, the HU_{mean} value increased (−841·78 ± 63 and −811·68 ± 49 for 0·625 and 3·75 mm, respectively). In a similar manner for the LEP, HU_{mean} values were 784·40 ± 44 and −781·29 ± 52 for 80 and 140 kV, respectively, which indicated an increase both with increasing kV and with slice thicknesses (−781·29 ± 56 and −748·82 ± 47 for 0·625 and 3·75 mm, respectively). According to these results, the change in HU_{mean} value according to slice thicknesses is more significant and implies the importance of thinner slice thicknesses in planning CT scans.

The calculated absorbed dose values on calculation points (CP) A and B for multiple fields and different photon energies (6 and 18 MV) were shown in Table 1–3 in the water-phantom, LEP and LIP, respectively. At the same time, both the superposition and convolution algorithms were used for dose calculations on the CT images taken at different tube voltages and slice thicknesses. As shown in Table 1, the maximum difference between the two algorithms for water was 0·7%. However, in the presence of an
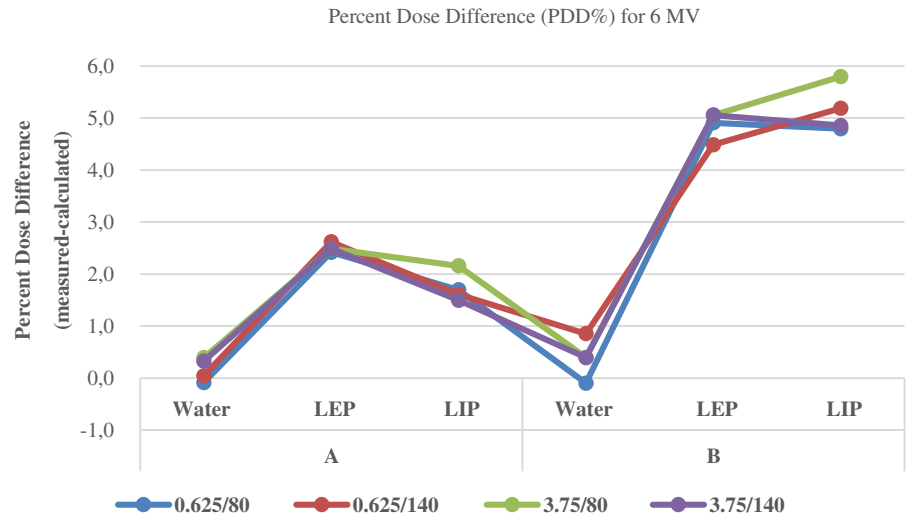
Percent Dose Difference (PDD%) for 6 MV

Figure 2. The percent dose difference between the measured and calculated absorbed doses at both points A and B for tube voltages and slice thicknesses with 6 MV.
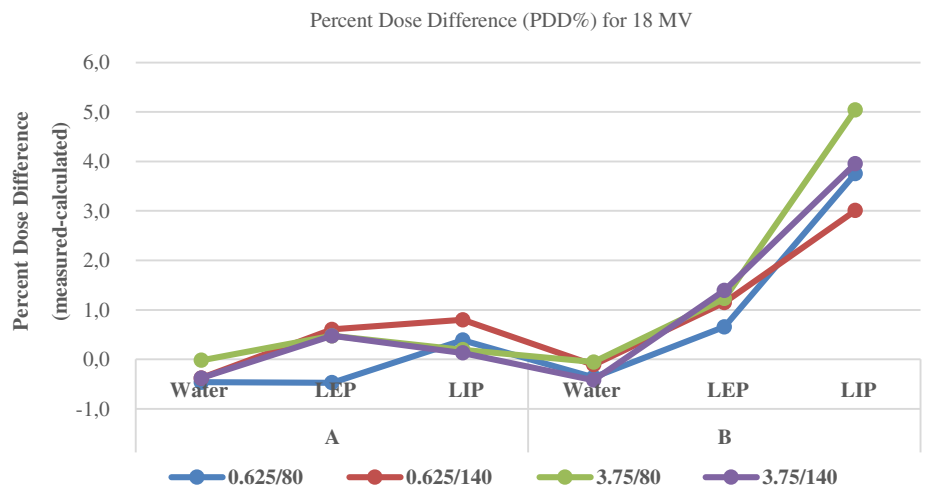
Percent Dose Difference (PDD%) for 18 MV

Figure 3. The percent dose difference between the measured and calculated absorbed doses at both points A and B for tube voltages and slice thicknesses with 18 MV.

inhomogeneous structure, the convolution algorithm seems to be insufficient as shown in Tables 2 and 3. The highest difference between the algorithms was 7·22 and 10·93% for 6 MV and 18 MV, respectively, in the calculation at point B of the LIP phantom.

CT scans for respiratory phases are very important in the treatment planning of lung regions.[9] In this study, the calculated maximum dose difference at point B between LEP and LIP was 1·00% for 6 MV and 2·80% for 18 MV. Also, the maximum dose difference at point A between LEP and LIP was 1·02 and 1·70% for 6 MV and 18 MV, respectively. This result shows that the absorbed dose was affected by the difference between the maximum inhalation and exhalation phase, especially at high energies.

The measured and calculated absorbed dose differences at both points A and B each of tube voltage and slice thickness for 6 MV were shown in Figure 2. The measured and calculated dose differences according to the tube voltage and slice thickness were very low in the water. The highest difference was 0·4% at point A and 0·9% at point B. The maximum difference between the calculated and the measured absorbed dose values of LIP was 5·49% at point B for 3·75 mm and 80 kV. For both LEP and LIP, the variations in absorbed dose according to the slice thicknesses and tube voltages were calculated. For both energies, the calculated doses at point B have shown that the absorbed dose value increased as the

slice thickness increased. The maximum increase was found to be 1·23% at 18 MV for LIP. All other differences of absorbed doses calculated were less than 1%.

The difference between the measured and calculated absorbed doses at both points A and B for tube voltages and slice thicknesses with 18MV were shown in Figure 3 where one may notice that the measured and calculated dose differences for different tube voltages and slice thicknesses were very low in the water. The highest differences were found to be 0·5% at point A and 0·4% at point B. The maximum difference between the calculated and measured absorbed dose values of LIP were 5·00% at point B for 3·75 mm and 80 kV.

Discussion

In the modern radiotherapy era, TPS algorithms considering inhomogeneous structures were introduced by with Batho[10] and inhomogeneity correction has become an important part of treatment planning especially in intensity-modulated radiation therapy (IMRT).[11] Implicating advanced algorithms in treatment planning that are based on Monte Carlo modelling such as convolution, superposition and collapse cone has improved the accuracy of dose

calculation in radiotherapy.[12–14] However, the plans usually need determination of EDs from CT data to account for the effects of inhomogeneity.[14] A CT number–ED calibration curve must be established to correlate the CT values with the corresponding ED values before planning on CT slices. The HU value is 0 for water and −1000 for air at standard temperature and pressure.

The CT number, in contrast, depends on the beam energy, density and number of atoms, as well as the attenuation property of the medium.[15] In addition, the CT number for a particular tissue is not constant and the tube voltage is related to the field of view. Therefore, one should be aware of the impact of these changes while treatment planning, since a different CT number may be given to the same tissue. Depending on the different scanning parameters, many researchers report changes in the CT number,[16–18] and some studies have been conducted to investigate the dosimetric effects of non-homogeneous cubic or anthropomorphic phantoms.[19,20] Consistent with this study, the effect of CT voltage kV on inhomogeneity in low atomic structures was reported to be clinically insignificant.[21] Recently, Zurl et al.[22] compared CT parameters and showed that changes in HU could be as large as 20%. However, the effect on the dose is limited with 1·5%. Ebert et al.[23] provided variability in the CT number in various settings and tube currents. It has been shown that the tube current (mA) does not play a role and CT number is affected only with kV. As we reported in this study, the differences between CT numbers and tube voltages were minimal, between 0·3 (lung) and 1·0 (water) in the density region.

The convolution algorithms have TERMA (total energy released per unit mass) and Kernel (a cumulative dose-spread array of photons interacting in a single point in the medium) components. The primary Kernel calculates the primary dose and the scatter kernel calculates the first and multiple scatter doses. The dose at any point can be calculated from the convolution of the TERMA with the kernel. In order to account tissue heterogeneities in a patient, kernel is scaled by radiological distances which are calculated from the material densities defined by CT images. For this reason, the superposition algorithms compute the dose by convolving the total energy released in the medium, with Monte Carlo-generated energy deposition kernels. Especially in regions with low density, the superposition algorithm must be used. In the study, there were no differences in the algorithms for the doses taken in the water equivalent phantoms, but it was found that the superposition algorithm calculated more accurate results for both LEP and LIP regions. In addition, according to the results of this study, appropriate dose evaluation should be made for both maximum inhalation and exhalation periods. Because, the difference between two periods may become significant especially when the doses higher than tolerance, are reached the organs at risk.

In conclusion, the dose to the lung is becoming more important to consider at high-dose and small-field applications such as IMRT and stereotactic body radiation therapy. In this study, high-accuracy dose validation using CT images was performed with phantoms prepared using lung equivalent cork. It is thought that the phantoms prepared in accordance with maximum and minimum respiratory phases can be a simple and inexpensive method to investigate any difference in the dosimetry of lung regions. This study was carried out for the absolute dose at a certain point along the central axis. In order to see any change in dose outside the axis, it is recommended that similar studies should include film measurements and Monte Carlo simulations which are the limitations of this study.

Author ORCIDs. Aysun Inal 0000-0002-1647-9787

References

1. Karimi R, Tornling G, Forsslund H et al. Lung density on high resolution computer tomography (HRCT) reflects degree of inflammation in smokers. Respir Res 2014; 15 (1): 23–33. doi:10.1186/1465-9921-15-23.

2. Fraass B, Doppke K, Hunt M et al. American Association of Physicists in Medicine Radiation Therapy Committee Task Group 53: quality assurance for clinical radiotherapy treatment planning. Med Phys 1998; 25 (10): 1773–1829. doi :10.1118/1.598373

3. Ma C M, Jiang S B, Pawlicki T et al. A quality assurance phantom for IMRT dose verification. Phys Med Biol 2003; 48 (5): 561–572. doi:10.1088/0031-9155/48/5/301

4. Ravichandran R, Binukumar J P, Sivakumar S S, Krishnamurthy K, Davis C A A method for estimation of accuracy of dose delivery with dynamic slit windows in medical linear accelerators. J Med Phys 2008; 33: 127–129. doi:10.4103/0971-6203.42768

5. Chang K P, Hung S H, Chie Y H, Shiau A C, Huang R J A comparison of physical and dosimetric properties of lung substitute materials. J Med Phys 2012; 39 (4): 2013–2020. doi:10.1118/1.3694097

6. Cloutier R J Tissue substitutes in radiation dosimetry and measurement. Radiat Res 1989; 119 (3): 582.doi:10.2307/3577533.

7. Hurkmans C W, van Lieshout M, Schuring D et al. Quality assurance of 4D-CT scan techniques in multicenter phase III trial of surgery versus stereotactic radiotherapy (Radiosurgery or Surgery for operable early stage (Stage 1A) non-small-cell Lung cancer [Rosel] Study). Int J Radiat Oncol Biol Phys 2011; 80 (3): 918–927. doi:10.1016/j.ijrobp.2010.08.017.

8. Aarup L R, Nahum A E, Zacharatou C et al. The effect of different lung densities on the accuracy of various radiotherapy dose calculation methods: implications for tumour coverage. Radiother Oncol 2009; 91: 405–414.doi:10.1016/j.radonc.2009.01.008.

9. Lee J J, Kim N, Seo J B, Lee H, Shin Y G. Automatic non-rigid lung registration method for the visualization of regional air trapping in chest CT scans. *Proceedings of the 11th International Conference on Medical Imaging Computing and Computer 10 Assisted Intervention MICCAI*, New York, NY, USA, September 6–10, 2008, pp. 195–201.

10. Batho H F Lung corrections in cobalt 60 beam therapy. J Can Assoc Radiol 1964; 15: 79–83.

11. Al-Hallaq H A, Reft C S, Roeske J C (2006) The dosimetric effects of tissue heterogeneities in intensity-modulated radiation therapy (IMRT) of the head and neck. Phys Med Biol 2006; 51 (5): 1145–1156. doi:10.1088/0031-9155/51/5/007.

12. Papanikolaou N, Battista J J, Boyer A L et al. Tissue inhomogeneity correction for megavoltage photon beams: Report of the Task Group No. 65 of the Radiation Therapy Committee of the American Association of Physicist in Medicine. AAPM Report No 85. Madison, WI: AAPM, 2004.

13. Ahnesjö A, Weber L, Murman A et al. Beam modeling and verification of a photon beam multisource model. Med Phys 2005; 32 (6): 1722–1737. doi:10.1118/1.1898485.

14. Knöös T, Ceberg C, Weber L, Nilsson P (1994) The dosimetric verification of a pencil beam based treatment planning system. Phys Med Biol 1994; 39 (10): 1609–1628. doi:10.1088/0031-9155/39/10/007

15. Watanabe Y Derivation of linear attenuation coefficients from CT numbers for low-energy photons. Phys Med Biol 1999; 44 (9): 2201–2211. doi:10.1088/0031-9155/44/9/308.

16. Groell R, Rienmueller R, Schaffler G J et al. CT number variations due to different image acquisition and reconstruction parameters: a thorax phantom study. Comput Med Imag Grap 2000; 24 (2): 53–58. doi:10.1016/s0895-6111(99)00043-9.

17. Kilby W, Sage J, Rabett V Tolerance levels for quality assurance of electron density values generated from CT in radiotherapy treatment planning. Phys Med Biol 2002; 47 (9): 1485–1492. doi:10.1088/0031-9155/47/9/304 18.

18. Millner M R, McDavid W D, Waggener R G et al. Extraction of information from CT scans at different energies. Med Phys 1979; 6 (1): 70–71. doi:10.1118/1.594555.

19. Cozzi L, Fogliata A, Buffa F, Bieri S Dosimetric impact of computed tomography calibration on a commercial treatment planning system for external radiation therapy. Radiother Oncol 1998; 48 (3): 335–338. doi:10.1016/s0167-8140(98)00072-3.

20. Guan H, Yin F F, Kim J H (2002) Accuracy of inhomogeneity correction in photon radiotherapy from CT scans with different settings. Phys Med Biol 2002; 47 (17): N223–N231. doi:10.1088/0031-9155/47/17/402.

21. Kendall R L, Gifford K A, Kirsner S M The impact of peak-kilovoltage settings on heterogeneity-corrected photon-beam treatment plans. Radiother Oncol 2006; 81 (2): 206–208. doi:10.1016/j.radonc.2006.10.005.

22. Zurl B, Tiefling R, Winkler P, Kindl P, Kapp K S Hounsfield units variations: impact on CT-density based conversion tables and their effects on dose distribution. Strahlenther Onkol 2014; 90 (1): 88–93. doi:10.1007/s00066-013-0464-523.

23. Ebert M A, Lambert J, Greer P B CT-ED conversion on a GE Lightspeed-RT scanner: influence of scanner settings. Australas Phys Eng Sci Med 2008; 31 (2): 154–159. doi:10.1007/bf03178591.